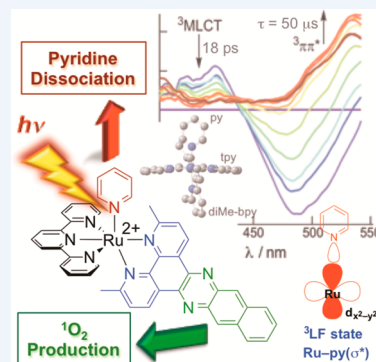


## New Ru(II) Complexes for Dual Photoreactivity: Ligand Exchange and $^1\text{O}_2$ Generation

Jessica D. Knoll, Bryan A. Albani, and Claudia Turro\*

Department of Chemistry and Biochemistry, The Ohio State University, Columbus, Ohio 43210, United States

**CONSPECTUS:** Uncovering the factors that govern the electronic structure of Ru(II)–polypyridyl complexes is critical in designing new compounds for desired photochemical reactions, and strategies to tune excited states for ligand dissociation and  $^1\text{O}_2$  production are discussed herein. The generally accepted mechanism for photoinduced ligand dissociation proposes that population of the dissociative triplet ligand field ( $^3\text{LF}$ ) state proceeds through thermal population from the vibrationally cooled triplet metal-to-ligand charge transfer ( $^3\text{MLCT}$ ) state; however, temperature-dependent emission spectroscopy provides varied activation energies using the emission and ligand exchange quantum yields for  $[\text{Ru}(\text{bpy})_2(\text{L})_2]^{2+}$  ( $\text{bpy} = 2,2'$ -bipyridine;  $\text{L} = \text{CH}_3\text{CN}$  or  $\text{py}$ ). This suggests that population of the  $^3\text{LF}$  state proceeds from the vibrationally excited  $^3\text{MLCT}$  state. Because the quantum yield of ligand dissociation for nitriles is much more efficient than that for  $\text{py}$ , steric bulk was introduced into the ligand set to distort the pseudo-octahedral geometry and lower the energy of the  $^3\text{LF}$  state. The  $\text{py}$  dissociation quantum yield with 500 nm irradiation in a series of  $[\text{Ru}(\text{tpy})(\text{NN})(\text{py})]^{2+}$  complexes ( $\text{tpy} = 2,2':6',2''$ -terpyridine;  $\text{NN} = \text{bpy}$ , 6,6'-dimethyl-2,2'-bipyridine ( $\text{Me}_2\text{bpy}$ ), 2,2'-biquinoline ( $\text{biq}$ )) increases by 2–3 orders of magnitude with the sterically bulky  $\text{Me}_2\text{bpy}$  and  $\text{biq}$  ligands relative to  $\text{bpy}$ . Ultrafast transient absorption spectroscopy reveals population of the  $^3\text{LF}$  state within 3–7 ps when  $\text{NN}$  is bulky, and density functional theory calculations support stabilized  $^3\text{LF}$  states. Dual activity via ligand dissociation and  $^1\text{O}_2$  production can be achieved by careful selection of the ligand set to tune the excited-state dynamics. Incorporation of an extended  $\pi$  system in Ru(II) complexes such as  $[\text{Ru}(\text{bpy})(\text{dppn})(\text{CH}_3\text{CN})_2]^{2+}$  ( $\text{dppn} = \text{benzo}[i]\text{dipyrido}[3,2-a:2',3'-c]\text{phenazine}$ ) and  $[\text{Ru}(\text{tpy})(\text{Me}_2\text{dppn})(\text{py})]^{2+}$  ( $\text{Me}_2\text{dppn} = 3,6$ -dimethylbenzo[*i*]dipyrido[3,2-*a*:2',3'-*c*]phenazine) introduces low-lying, long-lived  $\text{dppn}/\text{Me}_2\text{dppn}$   $^3\pi\pi^*$  excited states that generate  $^1\text{O}_2$ . Similar to  $[\text{Ru}(\text{bpy})_2(\text{CH}_3\text{CN})_2]^{2+}$ , photodissociation of  $\text{CH}_3\text{CN}$  occurs upon irradiation of  $[\text{Ru}(\text{bpy})(\text{dppn})(\text{CH}_3\text{CN})_2]^{2+}$ , although with lower efficiency because of the presence of the  $^3\pi\pi^*$  state. The steric bulk in  $[\text{Ru}(\text{tpy})(\text{Me}_2\text{dppn})(\text{py})]^{2+}$  is critical in facilitating the photoinduced  $\text{py}$  dissociation, as the analogous complex  $[\text{Ru}(\text{tpy})(\text{dppn})(\text{py})]^{2+}$  produces  $^1\text{O}_2$  with near-unit efficiency. The ability to tune the relative energies of the excited states provides a means to design potentially more active drugs for photochemotherapy because the photorelease of drugs can be coupled to the therapeutic action of reactive oxygen species, effecting cell death via two different mechanisms. The lessons learned about tuning of the excited-state properties can be applied to the use of Ru(II)–polypyridyl compounds in a variety of applications, such as solar energy conversion, sensors and switches, and molecular machines.



### INTRODUCTION

Excited states of Ru(II) complexes have been used in solar energy conversion,<sup>1–5</sup> in charge transfer reactions,<sup>6,7</sup> as sensors and switches,<sup>8,9</sup> and as potential therapeutic agents in photochemotherapy (PCT) and imaging.<sup>10–16</sup> Although many complexes are derived from  $[\text{Ru}(\text{bpy})_3]^{2+}$  ( $\text{bpy} = 2,2'$ -bipyridine) (Figure 1a),<sup>17</sup> these applications often have different demands. For example, the excited-state redox potential is crucial in solar energy schemes and charge transfer reactions, which often require long-lived triplet metal-to-ligand charge transfer ( $^3\text{MLCT}$ ) excited states, whereas strong luminescence and sensitivity to the environment have been important in sensor applications. In contrast, complexes developed for PCT typically require high yields of photoinduced ligand exchange for prodrug delivery or to achieve binding of the metal to biomolecules, which in turn results in short  $^3\text{MLCT}$  lifetimes with low luminescence yields. In order to tune the relative energies of the excited states to achieve the

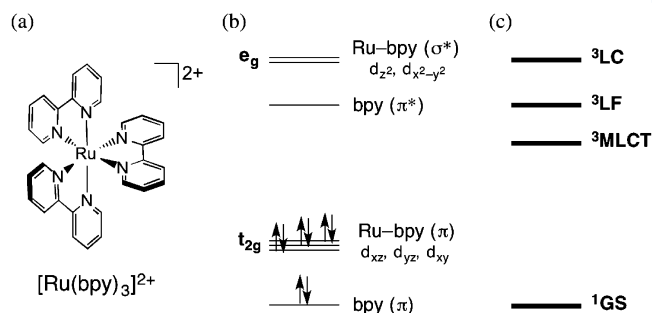


**Figure 1.** (a) Molecular structure and simplified (b) MO and (c) state diagrams of  $[\text{Ru}(\text{bpy})_3]^{2+}$ .

Received: April 22, 2015

Published: July 17, 2015

desired properties, an understanding of the factors that affect the electronic structure of Ru(II) complexes is necessary.

The electronic structure and excited-state dynamics of  $[\text{Ru}(\text{bpy})_3]^{2+}$  and related complexes have been the subject of numerous reviews.<sup>17</sup> Figure 1b presents a simplified diagram showing the frontier molecular orbitals (MOs) of  $[\text{Ru}(\text{bpy})_3]^{2+}$  in a pseudo-octahedral field, for which the lowest-energy  $^1\text{MLCT}$  transition has a maximum at 452 nm ( $\epsilon = 14\,600\text{ M}^{-1}\text{ cm}^{-1}$ ) and the bpy  $\pi\pi^*$  transitions are observed at 285 nm ( $\epsilon = 87\,000\text{ M}^{-1}\text{ cm}^{-1}$ ) in water.<sup>17</sup> Ultrafast  $^1\text{MLCT} \rightarrow ^3\text{MLCT}$  intersystem crossing (ISC) was reported in  $[\text{Ru}(\text{bpy})_3]^{2+}$  (15–40 fs),<sup>18,19</sup> and to our knowledge, significantly lower ISC rates have not been reported for Ru(II) complexes. Therefore, with the exception of charge injection into semiconductors,<sup>20</sup> the excited-state chemistry of Ru(II) complexes takes place from the triplet manifold. The low-lying triplet excited states of  $[\text{Ru}(\text{bpy})_3]^{2+}$  are schematically shown in Figure 1c, where the metal-centered triplet ligand field ( $^3\text{LF}$ ) state(s) involve transitions from the  $t_{2g}$ -type orbitals to the  $e_g$ -type orbitals, and the triplet ligand-centered ( $^3\text{LC}$ ) states arise from movement of an electron from the bpy( $\pi$ ) MOs to the bpy( $\pi^*$ ) MOs. In  $[\text{Ru}(\text{bpy})_3]^{2+}$ , the  $^3\text{MLCT}$  state is emissive ( $\lambda_{\text{em}} = 607\text{ nm}$ ,  $\tau = 620\text{ ns}$ ,  $\Phi = 0.042$  in water at 298 K).<sup>17</sup> The lifetimes of Ru(II) complexes in which the  $^3\text{LC}$  excited state falls below the  $^3\text{MLCT}$  state are similar to those of the  $^3\pi\pi^*$  state of the free ligand, and these complexes generally are not emissive, exhibit long lifetimes, and feature efficient  $^1\text{O}_2$  sensitization.<sup>21–24</sup> In contrast, stabilization of the  $^3\text{LF}$  states results in photoinduced ligand exchange, which may be accomplished by introducing distortions around the metal center. These distortions reduce the orbital overlap and lower the energy of the  $e_g$ -type orbitals,<sup>15</sup> thus decreasing the energy of the  $^3\text{LF}$  states, sometimes below that of the  $^3\text{MLCT}$  state.<sup>25</sup>

The present Account focuses on the effect of structural changes to ruthenium(II) complexes on the excited-state properties and reactivity. Of particular interest are compounds that undergo photoinduced ligand exchange and those that generate  $^1\text{O}_2$ , as well as new complexes designed in such a way that both processes are operative in the same complex upon irradiation with low-energy light. This dual reactivity has the potential to be useful in applications related to PCT, where cell death may be achieved via two different mechanisms by the same molecule.

## ■ ACTIVATION BARRIER TO PHOTOINDUCED LIGAND EXCHANGE

It is well-established that deactivation of the emissive  $^3\text{MLCT}$  state in Ru(II) complexes proceeds via thermal population of the  $^3\text{LF}$  states, which reduces the lifetime of the former. For applications that require charge transfer or high luminescence quantum yields, researchers aim to maximize the gap between the  $^3\text{MLCT}$  and  $^3\text{LF}$  states, which minimizes deactivation through the latter. In contrast, maximizing photoinduced ligand exchange of ruthenium(II) complexes, such as in the release of active molecules to biological targets and to gain understanding of their function, to inhibit enzymes, and to generate reactive species that can covalently bind to DNA, requires efficient population of the dissociative  $^3\text{LF}$  states.<sup>11,13–15</sup> One limitation is the relatively low quantum yield of ligand exchange in some complexes.

It has been generally accepted that the formation of photosubstituted products in Ru(II)–polypyridyl complexes

proceeds through thermal population of the dissociative  $^3\text{LF}$  state(s) from the vibrationally cooled emissive  $^3\text{MLCT}$  state ( $^3\text{MLCT}_{v=0}$ ).<sup>26</sup> It is also established that deactivation of the emissive  $^3\text{MLCT}_{v=0}$  state proceeds via population of the low-lying  $^3\text{LF}$  state(s), as depicted in Figure 2a. If it is assumed that

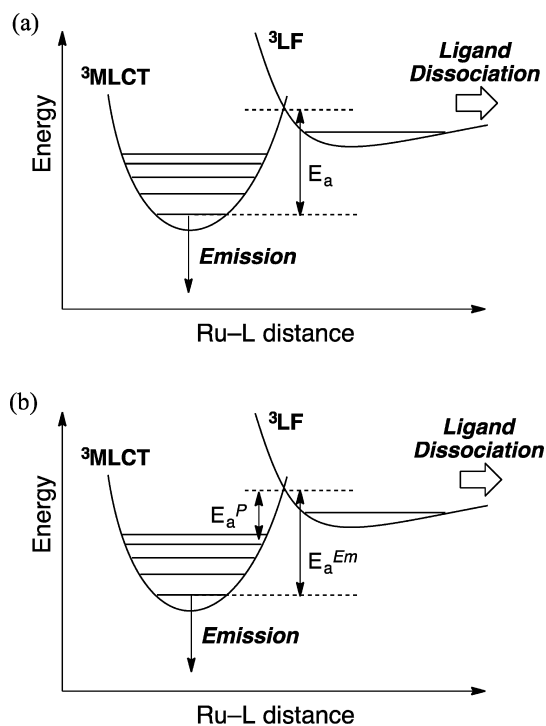


**Figure 2.** Schematic representation of the potential energy surfaces showing (a) the activation energy,  $E_a$ , for going from  $^3\text{MLCT}_{v=0}$  to the  $^3\text{LF}$  state and (b) the proposed sources of  $E_a^{\text{em}}$  and  $E_a^{\text{p}}$ .

the only source of photoinduced ligand exchange is population of the  $^3\text{LF}$  state from  $^3\text{MLCT}_{v=0}$ , then Arrhenius plots of both the photochemical yield and the emission intensity should give rise to the same activation energy,  $E_a$  (Figure 2a).

Plots of  $\ln(\Phi)$  versus  $1/T$  for the photoanation reactions of  $[\text{Ru}(\text{bpy})_2(\text{L})_2]^{2+}$  ( $\text{L} = \text{py}, \text{CH}_3\text{CN}$ ) to generate the corresponding  $[\text{Ru}(\text{bpy})_2(\text{L})\text{Cl}]^+$  product in the presence of excess tetrabutylammonium chloride (TBACl) in  $\text{CH}_2\text{Cl}_2$  were reported to result in  $E_a \approx 700\text{ cm}^{-1}$ ,<sup>27</sup> whereas changes in the emission lifetime of  $[\text{Ru}(\text{bpy})_2(\text{py})_2]^{2+}$  with temperature result in  $E_a = 2758\text{ cm}^{-1}$ .<sup>28</sup> However, these activation barriers were measured in two different temperature regimes, which can account for the different values. In addition, there have been other reports on the discrepancy between the magnitudes of  $E_a$  determined from emission and photochemical yields as well as from emission intensity and lifetime data.<sup>28,29</sup> The concluding remarks in both reports point to possible direct population of the  $^3\text{LF}$  state from the  $^1\text{MLCT}$  state together with population of the emissive  $^3\text{MLCT}$  state.<sup>28,29</sup>

To gain further understanding of the photoinduced ligand exchange in  $[\text{Ru}(\text{bpy})_2(\text{L})_2]^{2+}$  ( $\text{L} = \text{CH}_3\text{CN}, \text{py}$ ), the activation energies for photoanation to generate the corresponding complexes  $[\text{Ru}(\text{bpy})_2(\text{L})\text{Cl}]^+$ ,  $E_a^{\text{p}}$ , were measured over the same temperature range as for the value from the changes in emission intensity,  $E_a^{\text{em}}$ , in 4:1 ethanol/methanol above the glass transition temperature.<sup>30</sup> The experiments were conducted in a cryostat placed in the sample compartment of the fluorimeter, and the decrease in the emission intensity as the

temperature was raised was monitored in the absence of anion immediately after excitation to determine  $E_a^{\text{Em}}$ . The change in emission intensity as a function of irradiation time in the presence of 20 mM TBACl was used to calculate the value of  $E_a^{\text{P}}$ , and the results are listed in Table 1.<sup>30</sup> It is evident from

**Table 1. Quantum Yields of Photoinduced Ligand Exchange for  $[\text{Ru}(\text{bpy})_2(\text{L})_2]^{2+}$  Complexes, Absorption Maxima, and Activation Barriers with the Corresponding Temperature Ranges**

L	$\Phi_{\text{Cl}}^a$	$\lambda_{\text{abs}}/\text{nm}^b$	$E_a^{\text{Em}}/\text{cm}^{-1}{}^c$	$E_a^{\text{P}}/\text{cm}^{-1}{}^c$	T/K
$\text{CH}_3\text{CN}$	0.31	420	$1310 \pm 65$	$515 \pm 100$	130–170
py	0.17	460	$2040 \pm 100$	$940 \pm 85$	180–230

<sup>a</sup>At 25 °C in  $\text{CH}_2\text{Cl}_2$  with 20 mM TBACl ( $\lambda_{\text{irr}} = 400 \text{ nm}$ ). <sup>b</sup>In  $\text{H}_2\text{O}$ . <sup>c</sup>Irradiated at the absorption maximum.

Table 1 that for both complexes the value of  $E_a^{\text{P}}$  is significantly lower than that of  $E_a^{\text{Em}}$ . It may be concluded that the ligand exchange does not proceed from  ${}^3\text{MLCT}_{\nu=0}$ , as shown in Figure 2a. Instead, the population of the dissociative  ${}^3\text{LF}$  state must have a different origin, as previously proposed by us,<sup>31</sup> and may include direct ISC from the Franck–Condon  ${}^1\text{MLCT}$  state, internal conversion (IC) from a higher-energy  ${}^3\text{MLCT}$  state, or IC from the vibrationally excited lowest-energy  ${}^3\text{MLCT}$  state ( ${}^3\text{MLCT}_{\nu \gg 1}$ ). The latter situation is depicted in Figure 2b, where vibrational cooling competes with IC from a vibrational level well above  $\nu = 0$ , as previously proposed from ultrafast work.<sup>32</sup>

In order for efficient ligand dissociation to be observed, population of the  ${}^3\text{LF}$  state must compete with generation of  ${}^3\text{MLCT}_{\nu=0}$ . In systems such as  $[\text{Ru}(\text{bpy})_2(\text{CH}_3\text{CN})_2]^{2+}$ , there must be strong vibrational coupling between the MLCT (singlet or triplet) and  ${}^3\text{LF}$  states, which is reduced in  $[\text{Ru}(\text{bpy})_2(\text{py})_2]^{2+}$ . For example, strong vibrational coupling is believed to play a role in the ultrafast ISC of <100 fs in  $\text{Cr}(\text{acac})_3$  (acac = acetylacetonate), but interestingly, it decreases by over an order of magnitude when the ligand's peripheral methyl groups are replaced by *tert*-butyl substituents in  $\text{Cr}(t\text{-Bu-acac})_3$ .<sup>33</sup> In addition to nitriles, thioethers undergo photoinduced ligand dissociation with greater quantum yields than their ammine counterparts, and the  ${}^3\text{MLCT}$  states of the former were calculated to exhibit elongated Ru–S bonds, which may be related to MLCT/LF mixing.<sup>34</sup>

### ■ ENHANCED PHOTOINDUCED LIGAND EXCHANGE WITH STERIC BULK

To increase the quantum yield for pyridine exchange through enhanced population of the  ${}^3\text{LF}$  state, sterically bulky ligands were incorporated to distort the pseudo-octahedral geometry

around the metal center. The decrease in the energy of the  ${}^3\text{LF}$  state(s) as a function of increasing steric bulk was demonstrated for a series of complexes  $[\text{Ru}(\text{NN})_3]^{2+}$  with NN = bpy, 6-methyl-2,2'-bipyridine (6-Mebpy), and 4,4',6,6'-tetramethyl-2,2'-bipyridine ( $\text{Me}_4\text{bpy}$ ) using ultrafast transient absorption (TA) spectroscopy.<sup>25</sup> On the basis of the difference in the decay of the  ${}^3\text{MLCT}$  state and recovery of the ground state, it was shown that the rate of population of a  ${}^3\text{LF}$  state from the  ${}^3\text{MLCT}$  state increased by an order of magnitude in going from  $[\text{Ru}(6\text{-Mebpy})_3]^{2+}$  to the more sterically demanding  $[\text{Ru}(\text{Me}_4\text{bpy})_3]^{2+}$ , with  ${}^3\text{MLCT}$  lifetimes of 1.6 and 0.16 ps, respectively.<sup>25</sup> Distortions around the metal lead to a decrease in the calculated energy of the  ${}^3\text{LF}$  state by  $\sim 4000 \text{ cm}^{-1}$  in  $[\text{Ru}(6\text{-Mebpy})_3]^{2+}$  and  $\sim 7000 \text{ cm}^{-1}$  in  $[\text{Ru}(\text{Me}_4\text{bpy})_3]^{2+}$  relative to that in  $[\text{Ru}(\text{bpy})_3]^{2+}$ . Therefore, while the  ${}^3\text{LF}$  state lies above the  ${}^3\text{MLCT}$  state in the latter, it falls below the  ${}^3\text{MLCT}$  state in the former, resulting in fast  ${}^3\text{MLCT}$  decay to populate the  ${}^3\text{LF}$  state.

The enhanced population of the  ${}^3\text{LF}$  state(s) in ruthenium(II) complexes with bulky ligands leads to greater photoinduced ligand exchange. For example, photodissociation of 2,2'-biquinoline (biq) from  $[\text{Ru}(\text{biq})(\text{phen})_2]^{2+}$  (phen = 1,10-phenanthroline) and  $[\text{Ru}(\text{biq})_2(\text{phen})]^{2+}$  in  $\text{H}_2\text{O}$  occurs with  $\lambda_{\text{irr}} \geq 600 \text{ nm}$ , while this photoactivity is not observed in  $[\text{Ru}(\text{phen})_3]^{2+}$ .<sup>35</sup> The crystal structures of the biq complexes reveal lengthened Ru–N bonds compared with those in  $[\text{Ru}(\text{phen})_3]^{2+}$  as well as significant twisting of biq along the C–C bond connecting the two quinoline moieties and bending of biq by  $\sim 20^\circ$  out of the normal plane. Similar photoreactivity was reported for  $[\text{Ru}(\text{biq})_2(\text{bpy})]^{2+}$  in  $\text{CH}_3\text{CN}$ .<sup>36</sup> The presence of methyl, phenyl, or chloro substituents positioned toward the Ru(II) center also induces geometric distortions and facilitates photosubstitution of the bulky bidentate ligands with solvent molecules.<sup>15,37,38</sup>

To increase the photodissociation quantum yield of pyridine from pseudo-octahedral ruthenium(II) complexes, steric bulk was introduced in the series  $[\text{Ru}(\text{tpy})(\text{NN})(\text{py})]^{2+}$  (tpy = 2,2':6',2''-terpyridine; NN = bpy, 6,6'-dimethyl-2,2'-bipyridine ( $\text{Me}_2\text{bpy}$ ), biq) (Figure 3).<sup>39</sup> The lowest-energy electronic transition observed in  $[\text{Ru}(\text{tpy})(\text{NN})(\text{py})]^{2+}$  (NN = bpy,  $\text{Me}_2\text{bpy}$ ) is the  $\text{Ru}(d\pi) \rightarrow \text{tpy}(\pi^*)$   ${}^1\text{MLCT}$  transition with maxima at 468 nm ( $8120 \text{ M}^{-1} \text{ cm}^{-1}$ ) and 471 nm ( $8020 \text{ M}^{-1} \text{ cm}^{-1}$ ), respectively, whereas that in  $[\text{Ru}(\text{tpy})(\text{biq})(\text{py})]^{2+}$  is assigned as the  $\text{Ru}(d\pi) \rightarrow \text{biq}(\pi^*)$   ${}^1\text{MLCT}$  transition at 530 nm ( $9020 \text{ M}^{-1} \text{ cm}^{-1}$ ). Photoinduced exchange of py is not observed in  $[\text{Ru}(\text{tpy})(\text{bpy})(\text{py})]^{2+}$  ( $\Phi_{500} < 0.0001$ ), but irradiation of  $[\text{Ru}(\text{tpy})(\text{Me}_2\text{bpy})(\text{py})]^{2+}$  and  $[\text{Ru}(\text{tpy})(\text{biq})(\text{py})]^{2+}$  in  $\text{CH}_3\text{CN}$  generates the corresponding products  $[\text{Ru}(\text{tpy})(\text{NN})(\text{CH}_3\text{CN})]^{2+}$  (NN =  $\text{Me}_2\text{bpy}$ , biq) with  $\Phi_{500} = 0.16(1)$  and  $0.033(1)$ , respectively (Table 2). All three

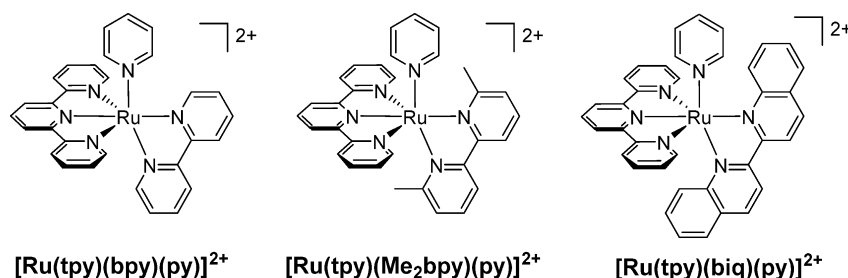


**Figure 3.** Structural representations of  $[\text{Ru}(\text{tpy})(\text{L})(\text{py})]^{2+}$  (NN = bpy,  $\text{Me}_2\text{bpy}$ , biq).

complexes are stable in CH<sub>3</sub>CN and H<sub>2</sub>O solutions in the dark for at least 24 h at room temperature.

**Table 2. Quantum Yields of Ligand Exchange,  $\Phi_{LE}$ , and  $^1O_2$  production,  $\Phi_{\Delta}$ , for Selected Complexes**

complex	$\Phi_{LE}^a$	$\Phi_{\Delta}^b$
[Ru(tpy)(bpy)(py)] <sup>2+</sup>	<10 <sup>-4</sup>	
[Ru(tpy)(Me <sub>2</sub> bpy)(py)] <sup>2+</sup>	0.16(1)	
[Ru(tpy)(biq)(py)] <sup>2+</sup>	0.033(1)	
[Ru(tpy)(dppn)(py)] <sup>2+</sup>	<10 <sup>-4</sup>	0.98(6)
[Ru(tpy)(Me <sub>2</sub> dppn)(py)] <sup>2+</sup>	0.053(1)	0.69(9)

<sup>a</sup>CH<sub>3</sub>CN,  $\lambda_{irr} = 500$  nm. <sup>b</sup>MeOH,  $\lambda_{irr} = 460$  nm.

The crystal structures reveal key structural distortions in [Ru(tpy)(Me<sub>2</sub>bpy)(py)]<sup>2+</sup> and [Ru(tpy)(biq)(py)]<sup>2+</sup> afforded by steric bulk from the bidentate ligands compared with [Ru(tpy)(bpy)(py)]<sup>2+</sup>. In particular, the angle between the plane defined by the bidentate ligand and that of the tpy ligand, determined to be 83.34° in [Ru(tpy)(bpy)(py)]<sup>2+</sup>, is reduced to 67.87° and 61.89° in [Ru(tpy)(Me<sub>2</sub>bpy)(py)]<sup>2+</sup> and [Ru(tpy)(biq)(py)]<sup>2+</sup>, respectively, similar to distortions reported for related complexes.<sup>35,40,41</sup> More importantly, the pyridine ligand in the Me<sub>2</sub>bpy and biq complexes is distorted relative to that in [Ru(tpy)(bpy)(py)]<sup>2+</sup>. The enhanced photoinduced ligand exchange efficiency is correlated to structural distortions, which are believed to stabilize <sup>3</sup>LF states and weaken the Ru–py  $\sigma$  bond.

Ultrafast TA spectroscopy reveals the consequences of added steric bulk on the excited-state dynamics of [Ru(tpy)(Me<sub>2</sub>bpy)(py)]<sup>2+</sup> compared with [Ru(tpy)(bpy)(py)]<sup>2+</sup> (Figure 4). For both complexes, the spectra feature a ground-state bleach centered at ~470 nm as well as positive transient absorption

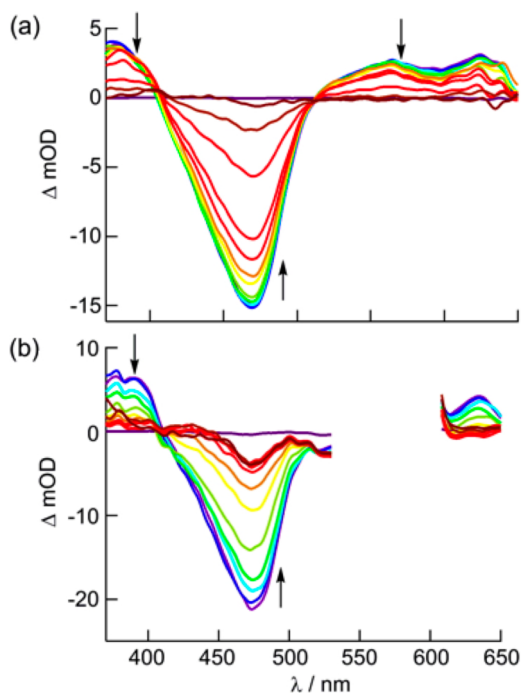


**Figure 4.** Transient absorption spectra of (a) [Ru(tpy)(bpy)(py)]<sup>2+</sup> ( $\lambda_{exc} = 350$  nm) and (b) [Ru(tpy)(Me<sub>2</sub>bpy)(py)]<sup>2+</sup> ( $\lambda_{exc} = 568$  nm) in CH<sub>3</sub>CN collected 1, 5, 10, 20, 40, 60, 100, 200, 500, 1000, and 2000 ps following the laser pulse (fwhm = 300 fs, baseline collected at -10 ps).

signals at ~375 and >500 nm associated with the Ru( $d\pi$ ) → tpy( $\pi^*$ ) <sup>3</sup>MLCT state.<sup>42</sup> While the spectral features are similar for the two complexes, stark differences are observed in the kinetics. The absorption changes of the bleach signal at 470 nm for [Ru(tpy)(bpy)(py)]<sup>2+</sup> in CH<sub>3</sub>CN (Figure 4a) can be fitted to a biexponential decay with  $\tau_1 = 28$  ps (8%) and  $\tau_2 = 544$  ps (92%). The absorption changes associated with the reduced ligands in the <sup>3</sup>MLCT states in the 350–420 nm range display a broad maximum at ~370 nm at 1–10 ps delay but sharpen and red-shift to ~375 nm with a shoulder at ~390 nm at later times. These changes are accompanied by biexponential decays at 375 and 575 nm with  $\tau_1 \approx 3$  ps and a long component with  $\tau_2 \approx 500$  ps. The Ru → bpy <sup>1</sup>MLCT state is preferentially excited at 350 nm, resulting in fast ISC to the corresponding Ru → bpy <sup>3</sup>MLCT state with maximum at ~370 nm associated with reduced bpy. This state decays to populate the Ru → tpy <sup>3</sup>MLCT state within ~23 ps, with a maximum at ~375 nm and a shoulder at ~410 nm, similar to the spectral features for [Ru(tpy)<sub>2</sub>]<sup>2+</sup>.<sup>43,44</sup> Since the 28 ps component represents a minor fraction (8%) of the bleach recovery, it corresponds to changes in absorption during <sup>3</sup>MLCT(bpy) → <sup>3</sup>MLCT(tpy) IC. The 23 ps component for the <sup>3</sup>MLCT(bpy) → <sup>3</sup>MLCT(tpy) IC is consistent with the value of 26 ps previously reported for a related complex with two low-lying <sup>3</sup>MLCT states.<sup>45</sup>

Excitation of the red edge of the Ru → tpy <sup>1</sup>MLCT absorption band of [Ru(tpy)(bpy)(py)]<sup>2+</sup> with  $\lambda_{exc} = 568$  nm produces a bleach signal that can be fitted to  $\tau_1 = 6$  ps (12%) and  $\tau_2 = 437$  ps (88%); similar kinetics are observed at 375 nm. The 6 ps component is attributed to vibrational relaxation in the Ru → tpy <sup>3</sup>MLCT state, which then decays to regenerate the ground state with  $\tau = 470$  ps (Figure 5a). As expected, the 23–28 ps component is not present with 568 nm excitation. The 470 ps lifetime of the Ru → tpy <sup>3</sup>MLCT state compares well to those of [Ru(tpy)<sub>2</sub>]<sup>2+</sup> (120 ps in CH<sub>3</sub>CN and 250 ps in H<sub>2</sub>O).<sup>42–44</sup>

The TA spectra that result from 568 nm excitation of [Ru(tpy)(Me<sub>2</sub>bpy)(py)]<sup>2+</sup> are shown in Figure 4b, where selective population of the Ru → tpy <sup>1</sup>MLCT state results in observation of the Ru → tpy <sup>3</sup>MLCT absorption signals at ~375 and ~400 nm with monoexponential decay of  $\tau = 6$  ps and a biexponential bleach recovery at 470 nm with  $\tau_1 = 7$  ps (16%) and  $\tau_2 = 38$  ps (84%). The 6–7 ps component can be ascribed to IC from the Ru → tpy <sup>3</sup>MLCT state to populate the <sup>3</sup>LF state, which competes with vibrational cooling in the former, and the <sup>3</sup>LF state regenerates the ground state with time constant of 38 ps (Figure 5b). Excitation of [Ru(tpy)(Me<sub>2</sub>bpy)(py)]<sup>2+</sup> at 350 nm provides similar kinetics but with an additional ~3 ps component associated with decay of the Ru → Me<sub>2</sub>bpy <sup>3</sup>MLCT state (Figure 5b). These experiments are consistent with generation of the <sup>3</sup>LF state within 3–7 ps, which then deactivates via ligand dissociation and thermal decay to the ground state. It is evident in the ultrafast TA data for [Ru(tpy)(Me<sub>2</sub>bpy)(py)]<sup>2+</sup> in Figure 4b that the ground state does not fully recover in the final trace (2 ns), consistent with formation of the monosubstituted CH<sub>3</sub>CN photoproduct, [Ru(tpy)(Me<sub>2</sub>bpy)(CH<sub>3</sub>CN)]<sup>2+</sup>. However, the kinetics of the photoproduct formation cannot be determined because of its spectral overlap with the ground and excited states of the starting compound and the relatively small quantity of photoproduct formed.

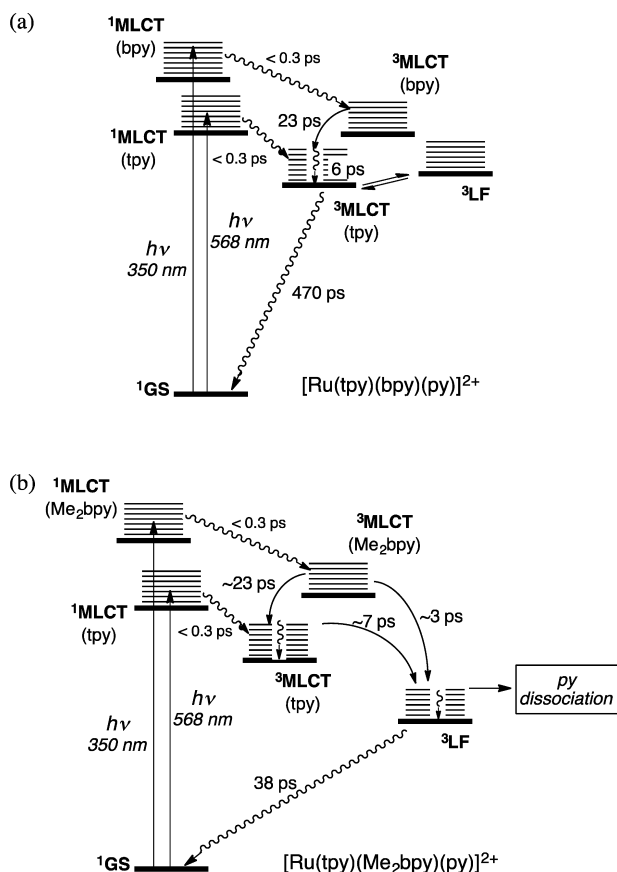


**Figure 5.** Jablonski diagrams for (a)  $[\text{Ru}(\text{tpy})(\text{bpy})(\text{py})]^{2+}$  and (b)  $[\text{Ru}(\text{tpy})(\text{Me}_2\text{bpy})(\text{py})]^{2+}$ .

Distortions around the metal center in  $[\text{Ru}(\text{tpy})(\text{Me}_2\text{bpy})(\text{py})]^{2+}$  compared with  $[\text{Ru}(\text{tpy})(\text{bpy})(\text{py})]^{2+}$  can explain the differences in excited-state dynamics, resulting in a lower-energy  ${}^3\text{LF}$  state in the former that falls below the  $\text{Ru} \rightarrow \text{tpy}$   ${}^3\text{MLCT}$  state (Figure 5). The lower-energy  ${}^3\text{LF}$  state leads to enhanced ligand exchange for the  $\text{Me}_2\text{bpy}$  complex; the  ${}^3\text{LF}$  lifetime of  $[\text{Ru}(\text{tpy})(\text{Me}_2\text{bpy})(\text{py})]^{2+}$  is similar to those of  $\text{Ru}(\text{II})$  complexes with sterically bulky ligands, 45 ps for  $[\text{Ru}(\text{6-Mebpy})_3]^{2+}$  and 7.5 ps for  $[\text{Ru}(\text{Me}_2\text{bpy})_3]^{2+}$ .<sup>25</sup> The formation of a pentacoordinate intermediate (PCI) from the  ${}^3\text{LF}$  state is possible, such that the dynamics of the ground-state regeneration are due to geminate recombination of the PCI and pyridine. However, the cage escape and geminate recombination kinetics for the related complex  $[\text{Ru}(\text{bpy})_2(\text{NA})_2]^{2+}$  ( $\text{NA} = \text{nicotinamide}$ ) in water were reported as 377 and 263 ps, respectively.<sup>32</sup> This order of magnitude difference between the bleach recovery of  $[\text{Ru}(\text{tpy})(\text{Me}_2\text{bpy})(\text{py})]^{2+}$  and  $[\text{Ru}(\text{bpy})_2(\text{NA})_2]^{2+}$  is inconsistent with the 38 ps component assigned as geminate recombination. Ultrafast population of the  ${}^3\text{LF}$  state from the  $\text{Ru} \rightarrow \text{tpy}$   ${}^1\text{MLCT}$  or vibrationally excited  ${}^3\text{MLCT}$  state,  ${}^3\text{MLCT}_{\text{vib}}$ , to afford py dissociation is supported by efficient ligand exchange for  $[\text{Ru}(\text{tpy})(\text{Me}_2\text{bpy})(\text{py})]^{2+}$  with low-energy light ( $\lambda_{\text{irr}} \geq 600$  nm) and the excited-state dynamics measured with 568 nm excitation. This finding is also consistent with the differences in  $E_a^{\text{Em}}$  and  $E_a^{\text{p}}$  measured for  $[\text{Ru}(\text{bpy})_2(\text{py})_2]^{2+}$  (Table 1).

Density functional theory (DFT) calculations on  $[\text{Ru}(\text{tpy})(\text{NN})(\text{py})]^{2+}$  ( $\text{NN} = \text{bpy}, \text{Me}_2\text{bpy}$ ) show that the unoccupied  $d_{x^2-y^2}$  orbital, directed along the  $\text{Ru}-\text{py}$  bond, is at a lower energy than the  $d_z^2$  orbital in each complex. Therefore,

population of the lowest-energy LF state results in additional electron density in the  $d_{x^2-y^2}$  orbital, weakening the  $\text{Ru}-\text{py}$  bond. The distortions in  $[\text{Ru}(\text{tpy})(\text{Me}_2\text{bpy})(\text{py})]^{2+}$  lower the calculated  $d_{x^2-y^2}$  orbital energy by 0.82 eV relative to  $[\text{Ru}(\text{tpy})(\text{bpy})(\text{py})]^{2+}$ , consistent with stabilization of the LF states with  $\text{Ru}-\text{py}(\sigma^*)$  character.

## DUAL ACTIVITY: PHOTOINDUCED LIGAND EXCHANGE AND ${}^1\text{O}_2$ GENERATION

$[\text{Ru}(\text{bpy})(\text{dppn})(\text{CH}_3\text{CN})_2]^{2+}$  ( $\text{dppn} = \text{benzo}[i]\text{dipyrido}[3,2-a:2',3'-c]\text{phenazine}$ ) (Figure 6) combines the ligand exchange

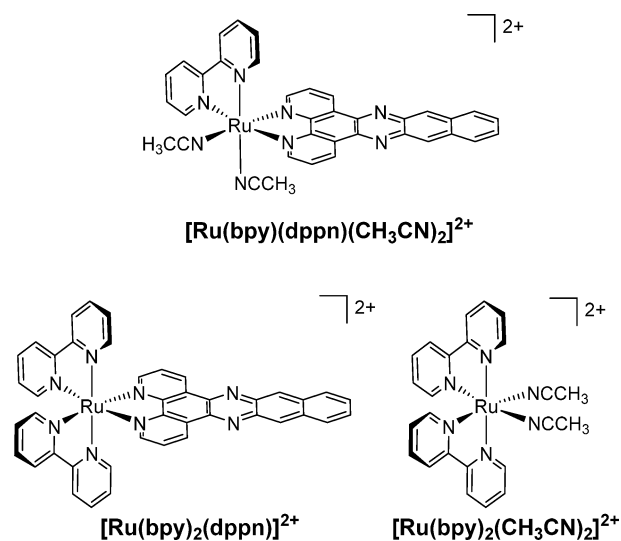


**Figure 6.** Structural representations of  $[\text{Ru}(\text{bpy})(\text{dppn})(\text{CH}_3\text{CN})_2]^{2+}$ ,  $[\text{Ru}(\text{bpy})_2(\text{dppn})]^{2+}$ , and  $[\text{Ru}(\text{bpy})_2(\text{CH}_3\text{CN})_2]^{2+}$ .

photochemistry of  $[\text{Ru}(\text{bpy})_2(\text{CH}_3\text{CN})_2]^{2+}$  and the  ${}^1\text{O}_2$  production of  $[\text{Ru}(\text{bpy})_2(\text{dppn})]^{2+}$  to enhance cellular phototoxicity.<sup>46</sup> The electronic absorption spectrum of  $[\text{Ru}(\text{bpy})(\text{dppn})(\text{CH}_3\text{CN})_2]^{2+}$  features a  ${}^1\text{MLCT}$  maximum at 430 nm ( $11\,000\text{ M}^{-1}\text{ cm}^{-1}$ ) and  $\text{dppn}$ -centered  ${}^1\pi\pi^*$  transitions at 382 nm ( $11\,100\text{ M}^{-1}\text{ cm}^{-1}$ ) and 405 nm ( $13\,500\text{ M}^{-1}\text{ cm}^{-1}$ ). The lowest-energy excited state of the complex is the  $\text{dppn}$ -centered  ${}^3\pi\pi^*$  state with  $\tau = 20\ \mu\text{s}$  in  $\text{CH}_3\text{CN}$ , similar to those of  $[\text{Ru}(\text{bpy})_2(\text{dppn})]^{2+}$  ( $\tau = 33\ \mu\text{s}$  in  $\text{CH}_3\text{CN}$ ) and free  $\text{dppn}$  ( $\tau = 18\ \mu\text{s}$  in  $\text{CHCl}_3$ ).<sup>21</sup> In  $[\text{Ru}(\text{bpy})_2(\text{CH}_3\text{CN})_2]^{2+}$ , both the lowest-energy  ${}^3\text{MLCT}$  excited state ( $\tau = 51\text{ ps}$ ) and the low-lying  ${}^3\text{LF}$  state are populated upon ultrafast excitation, and the complex undergoes efficient photoinduced ligand exchange.<sup>31</sup>

Irradiation of  $[\text{Ru}(\text{bpy})(\text{dppn})(\text{CH}_3\text{CN})_2]^{2+}$  in water promotes sequential substitution of the two  $\text{CH}_3\text{CN}$  ligands ( $\lambda_{\text{irr}} = 400\text{ nm}$ ); the first step forms  $[\text{Ru}(\text{bpy})(\text{dppn})(\text{CH}_3\text{CN})(\text{OH}_2)]^{2+}$  with  $\Phi_{400} = 0.002(3)$ , which is 2 orders of magnitude lower than that in  $[\text{Ru}(\text{bpy})_2(\text{CH}_3\text{CN})_2]^{2+}$  ( $\Phi_{400} = 0.21$ ).<sup>31</sup> The quantum yield for production of  ${}^1\text{O}_2$  ( $\Phi_{\Delta}$ ) from the  ${}^3\pi\pi^*$  state of  $[\text{Ru}(\text{bpy})(\text{dppn})(\text{CH}_3\text{CN})_2]^{2+}$  is 0.72(2), which is slightly lower than that of  $[\text{Ru}(\text{bpy})_2(\text{dppn})]^{2+}$  (0.88(2)). The lower yields of ligand exchange and  ${}^1\text{O}_2$  generation in  $[\text{Ru}(\text{bpy})(\text{dppn})(\text{CH}_3\text{CN})_2]^{2+}$  relative to the parent complexes are explained by competitive population of the  ${}^3\text{LF}$  and  ${}^3\pi\pi^*$  states. A phthalocyanine  $\text{Ru}(\text{II})$  complex with bound  $\text{NO}$  ligands was previously shown to produce  ${}^1\text{O}_2$  with  $\Phi_{\Delta} = 0.29$  and photorelease  $\text{NO}$ .<sup>47</sup>

Ultrafast TA spectroscopy reveals the excited-state dynamics of  $[\text{Ru}(\text{bpy})(\text{dppn})(\text{CH}_3\text{CN})_2]^{2+}$ . Because of spectral overlap

of the  $^1\text{MLCT}$  and  $^1\pi\pi^*$  bands, one cannot be accessed selectively. Excitation in the 300 to 400 nm range results in the observation of both the  $^3\text{MLCT}$  and  $^3\pi\pi^*$  states within the laser pulse, with absorption at  $\sim 360$  and  $\sim 540$  nm, respectively (Figure 7). Additionally, the lower-lying  $^3\pi\pi^*$  state is also

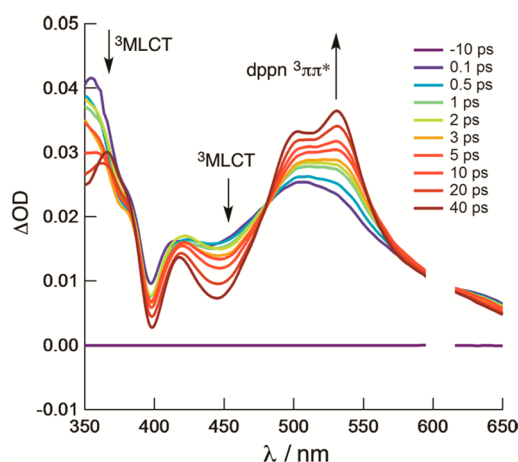


**Figure 7.** Transient absorption spectra of  $[\text{Ru}(\text{bpy})(\text{dppn})-(\text{CH}_3\text{CN})_2]^{2+}$  in  $\text{CH}_3\text{CN}$  ( $\lambda_{\text{exc}} = 300$  nm, fwhm = 300 fs).

populated from the  $^3\text{MLCT}$  state through IC with  $\tau = 22$  ps (Figure 7). Although the observed ligand exchange is expected to occur through the  $^3\text{LF}$  state, the latter was not detected, likely because of its low quantum yield and weak oscillator strength.

$[\text{Ru}(\text{tpy})(\text{Me}_2\text{dppn})(\text{py})]^{2+}$  ( $\text{Me}_2\text{dppn} = 3,6$ -dimethylbenzo- $[i]$ dipyrido[3,2- $a$ :2',3'- $c$ ]phenazine) (Figure 8) undergoes both

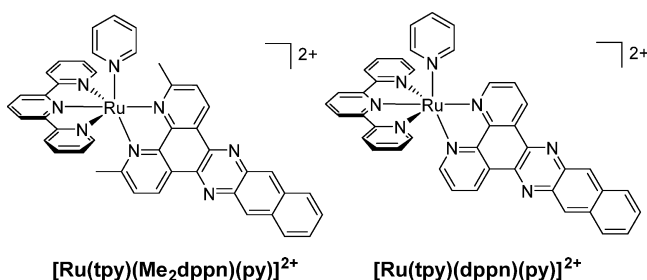


**Figure 8.** Structural representations of  $[\text{Ru}(\text{tpy})(\text{Me}_2\text{dppn})(\text{py})]^{2+}$  and  $[\text{Ru}(\text{tpy})(\text{dppn})(\text{py})]^{2+}$ .

pyridine dissociation and  $^1\text{O}_2$  production with visible light. The  $\text{Me}_2\text{dppn}$  ligand causes geometric strain similar to that caused by  $\text{Me}_2\text{bpy}$ , but the complex maintains the  $\text{Me}_2\text{dppn}$   $^3\pi\pi^*$  lowest-energy excited state.<sup>48</sup>  $[\text{Ru}(\text{tpy})(\text{Me}_2\text{dppn})(\text{py})]^{2+}$  absorbs strongly in the visible region with  $\text{dppn}$ -centered  $^1\pi\pi^*$  transitions at 382 nm ( $11\,400\ \text{M}^{-1}\ \text{cm}^{-1}$ ) and 404 nm ( $12\,400\ \text{M}^{-1}\ \text{cm}^{-1}$ ) and a  $^1\text{MLCT}$  peak at 486 nm ( $12\,900\ \text{M}^{-1}\ \text{cm}^{-1}$ ). When photolyzed in  $\text{CH}_3\text{CN}$  ( $\lambda_{\text{irr}} = 500$  nm),  $[\text{Ru}(\text{tpy})(\text{Me}_2\text{dppn})(\text{CH}_3\text{CN})]^{2+}$  is formed with  $\Phi_{500} = 0.053(1)$  in the absence of  $\text{O}_2$ , but ligand exchange is not observed in  $[\text{Ru}(\text{tpy})(\text{dppn})(\text{py})]^{2+}$  ( $\Phi_{500} < 10^{-4}$ ), which lacks steric strain (Table 2). Photosensitization of  $^1\text{O}_2$  by  $[\text{Ru}(\text{tpy})(\text{Me}_2\text{dppn})(\text{py})]^{2+}$  occurs with  $\Phi_{\Delta} = 0.69(9)$ , which is lower than the value of 0.98(6) measured for  $[\text{Ru}(\text{tpy})(\text{dppn})(\text{py})]^{2+}$  ( $\lambda_{\text{irr}} = 460$  nm), as listed in Table 2. The reduced quantum yield for  $[\text{Ru}(\text{tpy})(\text{Me}_2\text{dppn})(\text{py})]^{2+}$  can be attributed to competitive deactivation through the  $^3\text{LF}$  state afforded by

distortions around the metal. Competitive population of excited states also explains the lower ligand exchange quantum yield of  $[\text{Ru}(\text{tpy})(\text{Me}_2\text{dppn})(\text{py})]^{2+}$  relative to  $[\text{Ru}(\text{tpy})(\text{Me}_2\text{bpy})(\text{py})]^{2+}$ .

Following selective  $\text{Ru} \rightarrow \text{tpy}$   $^1\text{MLCT}$  excitation of  $[\text{Ru}(\text{tpy})(\text{dppn})(\text{py})]^{2+}$  and  $[\text{Ru}(\text{tpy})(\text{Me}_2\text{dppn})(\text{py})]^{2+}$  at 568 nm, the  $\text{Ru} \rightarrow \text{tpy}$   $^3\text{MLCT}$  state of  $[\text{Ru}(\text{tpy})(\text{Me}_2\text{dppn})(\text{py})]^{2+}$  is observed at  $\sim 390$  and  $\sim 415$  nm within the laser pulse, along with a strong ground-state bleach centered at  $\sim 480$  nm (Figure 9a). Although the signal at 535 nm corresponding

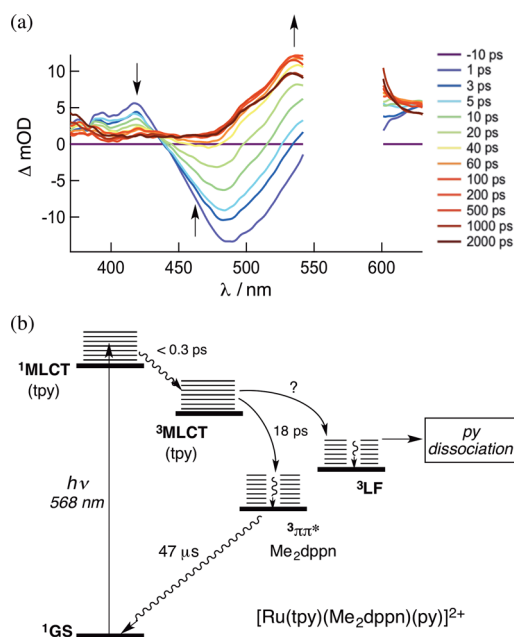


**Figure 9.** (a) Ultrafast transient absorption of  $[\text{Ru}(\text{tpy})(\text{Me}_2\text{dppn})(\text{py})]^{2+}$  in  $\text{CH}_3\text{CN}$  ( $\lambda_{\text{exc}} = 568$  nm, fwhm = 300 fs) and (b) the corresponding Jablonski diagram.

to the  $\text{Me}_2\text{dppn}$   $^3\pi\pi^*$  state is not observed at early times, it evolves with  $\tau_1 = 2$  ps (28%) and  $\tau_2 = 17$  ps (72%), concomitant with the decay of the  $^3\text{MLCT}$  signals fitted to  $\tau_1 = 3$  ps (13%) and  $\tau_2 = 18$  ps (87%) at 415 nm and changes in the bleach signal with  $\tau_1 = 1$  ps (16%) and  $\tau_2 = 18$  ps (84%). The  $\sim 2$  ps decay is believed to have contributions from ISC, IC, and vibrational cooling, while the 18 ps component is assigned to population of the  $^3\pi\pi^*$  state from the  $^3\text{MLCT}$  state. Similar spectral features and kinetics were measured for  $[\text{Ru}(\text{tpy})(\text{dppn})(\text{py})]^{2+}$  in  $\text{CH}_3\text{CN}$  under 568 nm excitation, for which the growth of the 540 nm peak and bleach recovery at 470 nm can be fitted to  $\tau_1 = 1$  ps (21%) and  $\tau_2 = 22$  ps (79%). The long component is ascribed to IC from the  $^3\text{MLCT}$  state to the  $\text{dppn}$   $^3\pi\pi^*$  state, while the short component is related to ISC, IC, and vibrational cooling processes.

The Jablonski diagram of  $[\text{Ru}(\text{tpy})(\text{Me}_2\text{dppn})(\text{py})]^{2+}$ , depicted in Figure 9b, shows that IC from the  $\text{Ru} \rightarrow \text{tpy}$   $^3\text{MLCT}$  state to the  $\text{dppn}$   $^3\pi\pi^*$  state occurs with  $\tau = 18$  ps in the  $\text{Me}_2\text{dppn}$  complex, as opposed to 22 ps in  $[\text{Ru}(\text{tpy})(\text{dppn})(\text{py})]^{2+}$ . Since photoinduced ligand exchange is observed in  $[\text{Ru}(\text{tpy})(\text{Me}_2\text{dppn})(\text{py})]^{2+}$  with  $\lambda_{\text{irr}} \geq 550$  nm, low-energy light must populate the dissociative  $^3\text{LF}$  state. The similarity in the  $^3\pi\pi^*$  lifetimes of  $[\text{Ru}(\text{tpy})(\text{dppn})(\text{py})]^{2+}$  and  $[\text{Ru}(\text{tpy})(\text{Me}_2\text{dppn})(\text{py})]^{2+}$  ( $\tau = 50$  and  $47\ \mu\text{s}$ , respectively;  $\lambda_{\text{exc}} = 355$  nm, fwhm  $\approx 8$  ns) is consistent with the  $^3\text{LF}$  state being located at a higher energy, as shown in Figure 9b.

## CONCLUSIONS

The ability of Ru(II) complexes to undergo both photoinduced ligand exchange and  $^1\text{O}_2$  generation efficiently provides a means to design potentially more active PCT therapeutics. In particular, photorelease of drugs can be coupled to the activity of reactive oxygen species, enabling these compounds to effect cell death via two different mechanisms upon visible-light irradiation. Steric strain can be used to lower the energy of the metal-centered state(s), resulting in greater yields of ligand photodissociation, even when these states(s) are not the lowest in energy. Mixing between the  $^3\text{LF}$  state(s) and MLCT and/or LC states is believed to play an important role in efficient photoinduced ligand exchange, which is greater when these states are closer in energy. Work is underway to gain further understanding of the coupling between states with the goal of increasing the ligand exchange yields in these dual-action complexes while retaining relatively high sensitization of  $^1\text{O}_2$  upon irradiation in the photodynamic window (600–900 nm).

## AUTHOR INFORMATION

### Corresponding Author

\*E-mail: turro.1@osu.edu.

### Notes

The authors declare no competing financial interest.

### Biographies

**Jessica D. Knoll** received her B.S. in chemistry from the University of Dayton in 2008. In 2013, she earned her Ph.D. from Virginia Tech with Prof. Karen Brewer, and she is currently a postdoctoral researcher with Prof. Claudia Turro at The Ohio State University.

**Bryan A. Albani** received his B.A. in chemistry from The College of Wooster in 2010. He obtained his Ph.D. in 2015 under the supervision of Prof. Claudia Turro at The Ohio State University and is employed as an Advanced Research Scientist at Owens Corning.

**Claudia Turro** was born in Argentina and received her B.S. and Ph.D. in chemistry at Michigan State University with Profs. Daniel Nocera and George Leroi. Her graduate work on ultrafast proton-coupled electron transfer and excited states of inorganic complexes was followed by research on the interactions of metal complexes with DNA at Columbia University with Prof. Nicholas Turro as a Jane Coffin Childs Memorial Fellow. She began her independent career as a faculty member at The Ohio State University in 1996.

## ACKNOWLEDGMENTS

The authors thank the National Science Foundation (CHE-1465067) and the National Institutes of Health (R01 EB16072) for partial support and the resources of the Center for Chemical and Biophysical Dynamics (CCBD) at OSU.

## REFERENCES

- (1) Serpone, N.; Pelizzetti, E.; Gratzel, M. Photosensitization of Semiconductors with Transition Metal Complexes – A Route to the Photoassisted Cleavage of Water. *Coord. Chem. Rev.* **1985**, *64*, 225–245.
- (2) Thompson, D. W.; Ito, A.; Meyer, T. J.  $[\text{Ru}(\text{bpy})_3]^{2+*}$  and Other Remarkable Metal-to-Ligand Charge Transfer (MLCT) Excited States. *Pure Appl. Chem.* **2013**, *85*, 1257–1305.
- (3) Zhang, Y.; Galoppini, E.; Johansson, P. G.; Meyer, G. J. Homoleptic Star-Shaped Ru(II) Complexes. *Pure Appl. Chem.* **2011**, *83*, 861–868.

(4) Kärkäs, M. D.; Johnston, E. V.; Verho, O.; Åkermark, B. Artificial Photosynthesis: From Nanosecond Electron Transfer to Catalytic Water Oxidation. *Acc. Chem. Res.* **2014**, *47*, 100–111.

(5) Hammarström, L. Accumulative Charge Separation for Solar Fuels Production: Coupling Light-Induced Single Electron Transfer to Multielectron Catalysis. *Acc. Chem. Res.* **2015**, *48*, 840–850.

(6) Hartings, M. R.; Kurnikov, I. V.; Dunn, A. R.; Winkler, J. R.; Gray, H. B.; Ratner, M. A. Electron Tunneling Through Sensitizer Wires Bound to Proteins. *Coord. Chem. Rev.* **2010**, *254*, 248–253.

(7) Anderson, B. L.; Maher, A. G.; Nava, M.; Lopez, N.; Cummins, C. C.; Nocera, D. G. Ultrafast Photoinduced Electron Transfer from Peroxide Dianion. *J. Phys. Chem. B* **2015**, *119*, 7422–7429.

(8) Lo, K. K.-W.; Li, S. P.-Y. Utilization of the Photophysical and Photochemical Properties of Phosphorescent Transition Metal Complexes in the Development of Photofunctional Cellular Sensors, Imaging Reagents, and Cytotoxic Agents. *RSC Adv.* **2014**, *4*, 10560–10585.

(9) King, A.; McClure, B. A.; Jin, Y.; Rack, J. J. Investigating the Effects of Solvent on the Ultrafast Dynamics of a Photoreversible Ruthenium Sulfoxide Complex. *J. Phys. Chem. A* **2014**, *118*, 10425–10432.

(10) Weidmann, A. G.; Komor, A. C.; Barton, J. K. Targeted Chemotherapy with Metal Complexes. *Comments Inorg. Chem.* **2014**, *34*, 114–123.

(11) Knoll, J. D.; Turro, C. Control and Utilization of Ruthenium and Rhodium Metal Complex Excited States for Photoactivated Cancer Therapy. *Coord. Chem. Rev.* **2015**, *282–283*, 110–126.

(12) Joshi, T.; Gasser, G. Towards Tris(diimine)-Ruthenium(II) and Bis(quinoline)-Re(I)(CO)<sub>3</sub> Complexes as Photoactivated Anticancer Drug Candidates. *Synlett* **2015**, *26*, 275–284.

(13) Barragan, F.; Lopez-Senin, P.; Salassa, L.; Betanzos-Lara, S.; Habtemariam, A.; Moreno, V.; Sadler, P. J.; Marchan, V. Photocontrolled DNA Binding of a Receptor-Targeted Organometallic Ruthenium(II) Complex. *J. Am. Chem. Soc.* **2011**, *133*, 14098–14108.

(14) Ford, P. C. Photochemical delivery of nitric oxide. *Nitric Oxide* **2013**, *34*, 56–64.

(15) Howerton, B. S.; Heidary, D. K.; Glazer, E. C. Strained Ruthenium Complexes Are Potent Light-Activated Anticancer Agents. *J. Am. Chem. Soc.* **2012**, *134*, 8324–8327.

(16) Shi, G.; Monro, S.; Hennigar, R.; Colpitts, J.; Fong, J.; Kasimova, K.; Yin, H.; DeCoste, R.; Spencer, C.; Chamberlain, L.; Mandel, A.; Lilge, L.; McFarland, S. A. Ru(II) Dyads Derived from  $\alpha$ -Oligothiophenes: A New Class of Potent and Versatile, Photosensitizers for PDT. *Coord. Chem. Rev.* **2015**, *282–283*, 127–138.

(17) (a) Campagna, S.; Puntoriero, F.; Nastasi, F.; Bergamini, G.; Balzani, V. Photochemistry and Photophysics of Coordination Compounds: Ruthenium. *Top. Curr. Chem.* **2007**, *280*, 117–214.

(b) McCusker, J. K. Femtosecond Transient Absorption Spectroscopy of Transition Metal Charge-Transfer Complexes. *Acc. Chem. Res.* **2003**, *36*, 876–887. (c) Juris, A.; Balzani, V.; Barigelletti, F.; Campagna, S.; Belser, P.; Von Zelewsky, A. Ru(II) Polypyridine Complexes: Photophysics, Photochemistry, Electrochemistry, and Chemiluminescence. *Coord. Chem. Rev.* **1988**, *84*, 85–277. (d) Kalyanasundaram, K. Photophysics, Photochemistry, and Solar Energy Conversion with Tris(bipyridyl)ruthenium(II) and Its Analogues. *Coord. Chem. Rev.* **1982**, *46*, 159–244.

(18) Cannizzo, A.; van Mourik, F.; Gawelda, W.; Zgrablic, G.; Bressler, C.; Chergui, M. Broadband Femtosecond Fluorescence Spectroscopy of  $[\text{Ru}(\text{bpy})_3]^{2+}$ . *Angew. Chem., Int. Ed.* **2006**, *45*, 3174–3176.

(19) Bhasikuttan, A. C.; Suzuki, M.; Nakashima, S.; Okada, T. Ultrafast Fluorescence Detection in Tris(2,2'-bipyridine)ruthenium(II) Complex in Solution: Relaxation Dynamics Involving Higher Excited States. *J. Am. Chem. Soc.* **2002**, *124*, 8398–8405.

(20) Anderson, N. A.; Lian, T. Ultrafast Electron Injection from Metal Polypyridyl Complexes to Metal-Oxide Nanocrystalline Thin Films. *Coord. Chem. Rev.* **2004**, *248*, 1231–1246.

(21) (a) Sun, Y.; Joyce, L.; Dickson, N. M.; Turro, C. Efficient DNA Photocleavage by  $[\text{Ru}(\text{bpy})_2(\text{dppn})]^{2+}$  with Visible Light. *Chem.*

*Commun.* **2010**, *46*, 2426. (b) Liu, Y.; Hammitt, R.; Lutterman, D. A.; Joyce, L. E.; Thummel, R. P.; Turro, C. Ru(II) Complexes of New Tridentate Ligands: Unexpected High Yield of Sensitized  $^1\text{O}_2$ . *Inorg. Chem.* **2009**, *48*, 375–385.

(22) Lincoln, R.; Kohler, L.; Monro, S.; Yin, H.; Stephenson, M.; Zong, R.; Chouai, A.; Dorsey, C.; Hennigar, R.; Thummel, R. P.; McFarland, S. A. Exploitation of Long-Lived  $^3\text{IL}$  Excited States for Metal-Organic Photodynamic Therapy: Verification in a Metastatic Melanoma Model. *J. Am. Chem. Soc.* **2013**, *135*, 17161–17175.

(23) Ford, W. E.; Rodgers, M. A. J. Reversible Triplet-Triplet Energy Transfer within a Covalently Linked Molecule. *J. Phys. Chem.* **1992**, *96*, 2917–2920.

(24) Gu, J.; Chen, J.; Schmehl, R. H. Using Intramolecular Energy Transfer to Transform non-Photoactive, Visible-Light-Absorbing Chromophores into Sensitizers for Photoredox Reactions. *J. Am. Chem. Soc.* **2010**, *132*, 7338–7346.

(25) Sun, Q.; Mosquera-Vazquez, S.; Daku, L. M. L.; Guenee, L.; Goodwin, H. A.; Vauthey, E.; Hauser, A. Experimental Evidence of Ultrafast Quenching of the  $^3\text{MLCT}$  Luminescence in Ruthenium(II) Tris-bipyridyl Complexes via a  $^3\text{dd}$  State. *J. Am. Chem. Soc.* **2013**, *135*, 13660–13663. (b) Sun, Q.; Mosquera-Vazquez, S.; Suffren, Y.; Hankache, J.; Amstutz, N.; Daku, L. M. L.; Vauthey, E.; Hauser, A. On the Role of Ligand-Field States for the Photophysical Properties of Ruthenium(II) Polypyridyl Complexes. *Coord. Chem. Rev.* **2015**, *282–283*, 87–99.

(26) (a) Malouf, G.; Ford, P. C. Photochemistry of the Ruthenium(II) Ammine Complexes,  $\text{Ru}(\text{NH}_3)_5(\text{py-X})^{2+}$ . Variation of Systemic Parameters to Modify Photochemical Reactivities. *J. Am. Chem. Soc.* **1977**, *99*, 7213–7221. (b) Tfouni, E. Photochemical Reactions of Ammineruthenium(II) Complexes. *Coord. Chem. Rev.* **2000**, *196*, 281–305.

(27) Pinnick, D. V.; Durham, B. Temperature Dependence of the Quantum Yields for the Photoanation of  $\text{Ru}(\text{bpy})_2(\text{L})^{2+}$  Complexes. *Inorg. Chem.* **1984**, *23*, 3841–3842.

(28) Wacholtz, W. M.; Auerbach, R. A.; Schmehl, R. H.; Ollino, M.; Cherry, W. R. Correlation of Ligand Field Excited State Energies with Ligand Field Strength in (Polypyridine)ruthenium(II) Complexes. *Inorg. Chem.* **1985**, *24*, 1758–1760.

(29) Durham, B.; Caspar, J. V.; Nagle, J. K.; Meyer, T. J. Photochemistry of  $\text{Ru}(\text{bpy})_3^{2+}$ . *J. Am. Chem. Soc.* **1982**, *104*, 4803–4810.

(30) Sgambellone, M. A. Photochemistry and Photophysics of Octahedral Ruthenium Complexes. Ph.D. Dissertation, The Ohio State University, Columbus, OH, 2013.

(31) Liu, Y.; Turner, D. B.; Singh, T. N.; Angeles-Boza, A. M.; Chouai, A.; Dunbar, K. R.; Turro, C. Ultrafast Ligand Exchange: Detection of a Pentacoordinate Ru(II) Intermediate and Product Formation. *J. Am. Chem. Soc.* **2009**, *131*, 26–27.

(32) Greenough, S. E.; Roberts, G. M.; Smith, N. A.; Horbury, M. D.; McKinlay, R. G.; Zurek, J. M.; Paterson, M. J.; Sadler, P. J.; Stavros, V. G. Ultrafast Photo-Induced Ligand Solvolysis of *cis*- $[\text{Ru}(\text{bipyridine})_2(\text{nicotinamide})_2]^{2+}$ : Experimental and Theoretical Insight into Its Photoactivation Mechanism. *Phys. Chem. Chem. Phys.* **2014**, *16*, 19141–19155.

(33) Schrauben, J. N.; Dillman, K. L.; Beck, W. F.; McCusker, J. K. Vibrational Coherence in the Excited State Dynamics of  $\text{Cr}(\text{acac})_3$ : Probing the Reaction Coordinate for Ultrafast Intersystem Crossing. *Chem. Sci.* **2010**, *1*, 405–410.

(34) Garner, R. N.; Joyce, L. E.; Turro, C. Effect of Electronic Structure on the Photoinduced Ligand Exchange of Ru(II) Polypyridine Complexes. *Inorg. Chem.* **2011**, *50*, 4384–4391.

(35) Wachter, E.; Heidary, D. K.; Howerton, B. S.; Parkin, S.; Glazer, E. C. Light-Activated Ruthenium Complexes Photobind DNA and are Cytotoxic in the Photodynamic Therapy Window. *Chem. Commun.* **2012**, *48*, 9649–9651.

(36) Von Zelewsky, A.; Gremaud, G. Ruthenium(II) Complexes with Three Different Diimine Ligands. *Helv. Chim. Acta* **1988**, *71*, 1108–1115.

(37) Laemmel, A.-C.; Collin, J.-P.; Sauvage, J.-P. Efficient and Selective Photochemical Labilization of a Given Bidentate Ligand in Mixed Ruthenium(II) Complexes of the  $\text{Ru}(\text{phen})_2\text{L}^{2+}$  and  $\text{Ru}(\text{bipy})_2\text{L}^{2+}$  Family (L = Sterically Hindering Chelate). *Eur. J. Inorg. Chem.* **1999**, 383–386.

(38) Baranoff, E.; Collin, J.; Furusho, J.; Furusho, Y.; Laemmel, A.; Sauvage, J. Photochemical or Thermal Chelate Exchange in the Ruthenium Coordination Sphere of Complexes of the  $\text{Ru}(\text{phen})_2\text{L}$  Family (L = Diimine or Dinitrile Ligands). *Inorg. Chem.* **2002**, *41*, 1215–1222.

(39) Knoll, J. D.; Albani, B. A.; Durr, C. B.; Turro, C. Unusually Efficient Pyridine Photodissociation from Ru(II) Complexes with Sterically Bulky Bidentate Ancillary Ligands. *J. Phys. Chem. A* **2014**, *118*, 10603–10610.

(40) Wachter, E.; Howerton, B. S.; Hall, E. C.; Parkin, S.; Glazer, E. C. A New Type of DNA “Light-Switch”: A Dual Photochemical Sensor and Metalating Agent for Duplex and G-Quadruplex DNA. *Chem. Commun.* **2014**, *50*, 311–313.

(41) Bonnet, S.; Collin, J.-P.; Sauvage, J.-P.; Schofield, E. Photochemical Expulsion of the Neutral Monodentate Ligand L in  $\text{Ru}(\text{Terpy}^*)(\text{Diimine})(\text{L})^{2+}$ : A Dramatic Effect of the Steric Properties of the Spectator Diimine Ligand. *Inorg. Chem.* **2004**, *43*, 8346–8354.

(42) Winkler, J. R.; Netzel, T. L.; Creutz, C.; Sutin, N. Direct Observation of Metal-to-ligand Charge-Transfer (MLCT) Excited States of Pentaammineruthenium(II) Complexes. *J. Am. Chem. Soc.* **1987**, *109*, 2381–2392.

(43) Siemeling, U.; Vor der Bruggen, J.; Vorfeld, U.; Neumann, B.; Stammeler, A.; Stammeler, H.; Brockhinke, A.; Plessow, R.; Zanello, P.; Laschi, F.; de Biani, F. F.; Fontani, M.; Steenken, S.; Stapper, M.; Gurzadyan, G. Ferrocenyl-Functionalised Terpyridines and Their Transition-Metal Complexes: Syntheses, Structures and Spectroscopic and Electrochemical Properties. *Chem. - Eur. J.* **2003**, *9*, 2819–2833.

(44) Liu, Y.; Hammitt, R.; Lutterman, D. A.; Thummel, R. P.; Turro, C. Marked Differences in Light-Switch Behavior of Ru(II) Complexes Possessing a Tridentate DNA Intercalating Ligand. *Inorg. Chem.* **2007**, *46*, 6011–6021.

(45) Sun, Y.; Liu, Y.; Turro, C. Ultrafast Dynamics of the Low-Lying  $^3\text{MLCT}$  States of  $[\text{Ru}(\text{bpy})_2(\text{dppp2})]^{2+}$ . *J. Am. Chem. Soc.* **2010**, *132*, 5594–5595.

(46) Albani, B. A.; Peña, B.; Leed, N. A.; de Paula, N. A. B. G.; Pavani, C.; Baptista, M. S.; Dunbar, K. R.; Turro, C. Marked Improvement in Photoinduced Cell Death by a New Tris-heteroleptic Complex with Dual Action: Singlet Oxygen Sensitization and Ligand Dissociation. *J. Am. Chem. Soc.* **2014**, *136*, 17095–17101.

(47) Carneiro, Z. A.; de Moraes, J. C. B.; Rodrigues, F. P.; de Lima, R. G.; Curti, C.; da Rocha, Z. N.; Paulo, M.; Bendhack, L. M.; Tedesco, A. C.; Formiga, A. L. B.; da Silva, R. S. Photocytotoxic activity of a nitrosyl phthalocyanine ruthenium complex – A system capable of producing nitric oxide and singlet oxygen. *J. Inorg. Biochem.* **2011**, *105*, 1035–1043.

(48) Knoll, J. D.; Albani, B. A.; Turro, C. Excited State Investigation of a New Ru(II) Complex for Dual Reactivity with Low Energy Light. *Chem. Commun.* **2015**, *51*, 8777–8780.